Sensors **2008**, *8*, 2136-2160

sensors

ISSN 1424-8220
© 2008 by MDPI
www.mdpi.org/sensors

Review

Relationship Between Remotely-sensed Vegetation Indices, Canopy Attributes and Plant Physiological Processes: What Vegetation Indices Can and Cannot Tell Us About the Landscape

Edward P. Glenn [1,*], Alfredo R. Huete [2], Pamela L. Nagler [3] and Stephen G. Nelson [4]

[1] Environmental Research Laboratory of the University of Arizona, 2601 E. Airport Drive, Tucson, AZ, USA 85706

[2] Terrestrial Biophysics and Remote Sensing Lab, Department of Soil, Water and Environmental Science, University of Arizona, Tucson, AZ, USA 85721; E-mail: ahuete@ag.arizona.edu

[3] U.S. Geological Survey, Southwest Biological Science Center, Sonoran Desert Research Center, University of Arizona, Tucson, AZ, USA 85721; E-mail: pnagler@usgs.gov

[4] Environmental Research Laboratory of the University of Arizona, 2601 E. Airport Drive, Tucson, AZ, USA 85706; E-mail: nsteve@ag.arizona.edu

* Author to whom correspondence should be addressed; E-mail: eglenn@ag.arizona.edu.

Received: 30 January 2008 / Accepted: 25 March 2008 / Published: 28 March 2008

Abstract: Vegetation indices (VIs) are among the oldest tools in remote sensing studies. Although many variations exist, most of them ratio the reflection of light in the red and NIR sections of the spectrum to separate the landscape into water, soil, and vegetation. Theoretical analyses and field studies have shown that VIs are near-linearly related to photosynthetically active radiation absorbed by a plant canopy, and therefore to light-dependent physiological processes, such as photosynthesis, occurring in the upper canopy. Practical studies have used time-series VIs to measure primary production and evapotranspiration, but these are limited in accuracy to that of the data used in ground truthing or calibrating the models used. VIs are also used to estimate a wide variety of other canopy attributes that are used in Soil-Vegetation-Atmosphere Transfer (SVAT), Surface Energy Balance (SEB), and Global Climate Models (GCM). These attributes include fractional vegetation cover, leaf area index, roughness lengths for turbulent transfer, emissivity and albedo. However, VIs often exhibit only moderate, non-linear

relationships to these canopy attributes, compromising the accuracy of the models. We use case studies to illustrate the use and misuse of VIs, and argue for using VIs most simply as a measurement of canopy light absorption rather than as a surrogate for detailed features of canopy architecture. Used this way, VIs are compatible with "Big Leaf" SVAT and GCMs that assume that canopy carbon and moisture fluxes have the same relative response to the environment as any single leaf, simplifying the task of modeling complex landscapes.

Keywords: Remote Sensing, NDVI, EVI, Evapotranspiration, Primary Production

1. Introduction

Vegetation indices (VIs) to monitor terrestrial landscapes by satellite sensors were first developed in the 1970s and have been highly successful in assessing vegetation condition, foliage, cover, phenology, and processes such as evapotranspiration (ET) and primary productivity, related to the fraction of photosynthetically active radiation absorbed by a canopy (fPAR) [1-3]. VIs are robust satellite data products computed the same way across all pixels in time and space, regardless of surface conditions. As ratios, they can be easily cross-calibrated across sensor systems, ensuring continuity of data sets for long-term monitoring of the land surface and climate-related processes. For example, there is a global record of Normalized Difference Vegetation Index (NDVI) data since 1981from the NOAA Advanced Very High Resolution Radiometer (AVHRR) that has contributed to global climate, ecosystem, and agricultural studies. A new generation of VI data from the Moderate Resolution Imaging Spectrometer (MODIS) on the Terra satellite has been inter-calibrated with AVHRR NDVI, and provides near daily coverage of the earth at 250 m pixel resolution [3].

Kerr and Ostrovsky [1] and Pettorelli *et al*. [2] have recently reviewed the numerous applications of satellite VIs in ecological studies. VIs are now indispensable tools in land cover classification, climate- and land-use-change detection, drought monitoring, and habitat loss, to name just a few applications. In this paper we briefly review the theoretical basis for VIs and give some examples of their use and misuse in two particular applications, estimating ecosystem carbon and moisture fluxes, important topics in global change studies.

Numerous studies have shown that satellite-derived VIs are optical measures of canopy "greenness", a composite property of leaf chlorophyll content, leaf area, canopy cover and structure. However, VIs have also been employed as proxies for individual, and often land-cover-dependent, vegetation parameters such as fractional vegetation cover (f_c), leaf area index (LAI), roughness lengths for turbulent transfer, albedo, emissivity and other biophysical properties of the landscape. These parameters are often required in Soil-Vegetation-Atmosphere Transfer (SVAT), Surface Energy Balance (SEB), and Global Climate Models (GCM) that attempt to predict surface fluxes based on physical models. Unfortunately, these canopy attributes are often only moderately correlated with VIs or their derivatives, and remote sensing models that use VIs to estimate these parameters are subject to error and uncertainty.

On the other hand, networks of flux towers now provide real-time, plot-level estimates of carbon assimilation and moisture and energy fluxes in major biome types around the world. We give recent examples in which VIs have been combined with data from flux towers and meteorological stations to accurately scale carbon and moisture fluxes over large landscape units, circumventing in some cases the need to solve complex SVAT or SEB equations with limited input data.

It seems surprising that VIs are so closely related to carbon and moisture fluxes, because fluxes are controlled in part by stomatal resistance, which can vary considerably over short time periods. However, over longer time periods (weeks or months), plants tend to adjust their foliage density to match the capacity of the environment to support photosynthesis (the Resource Optimization Theory) [4]. Leaves are expensive to produce and maintain, and when plants are nutrient-limited, water-stressed, or exposed to other unfavorable conditions, they reduce their leaf area to use resources efficiently, although full optimization is never achieved [5]. Hence, foliage density measured by time-series VIs can be a powerful tool in measuring the physiological status of vegetation.

Our goal is to point the way towards using VIs directly in scaling carbon and moisture fluxes rather than as proxies for canopy state attributes that are difficult to measure [6]. This is not a comprehensive review, as many dozens or hundreds of papers have been published on most of the topics covered. We have attempted to emphasize a few important historical papers, recent reviews, or recent papers that provide the reader an entry into literature on each topic. We illustrate the use and misuse of VIs with data from our studies of riparian vegetation in the southwestern U.S.

2. What VIs Measure

Although many different VIs have been formulated, most of them are related to the Simple Ratio (SR) [7]:

$$SR = \rho NIP/\rho Red \tag{1}$$

The most-used VI is the NDVI [1,3]:

$$NDVI = (\rho NIR - \rho Red)/(\rho NIR + \rho Red) \tag{2}$$

where ρNIR and ρRed are reflectance values of Red and Near Infrared light received at the sensors. The NDVI was first formulated by Rouse *et al.* [8] and applied to a wide range of practical remote sensing applications in a series of studies by Tucker and colleagues in the 1970s and 1980s, e.g. [9]. The SR and NDVI are built on the observation that chlorophylls a and b in green leaves strongly absorb light in the Red, with maximum absorption at about 690 nm, while the cell walls strongly scatter (reflect and transmit) light in the NIR region (about 850 nm) [10]. This results in a strong absorption contrast across a narrow wavelength band of 650 - 850 nm, captured by the NDVI and other VIs. NDVI and related VIs are functional variants of the SR. NDVI normalizes values between -1 to +1; dense vegetation has a high NDVI, while soil values are low but positive, and water is negative due to its strong absorption of NIR.

Tucker [10] tested various combinations of the red, NIR, and green bands to predict biomass, water content, and chlorophyll content of grass plots. The NDVI was strongly correlated with chlorophyll content and crop characteristics that were directly related to chlorophyll content, such as green biomass and leaf water content. Monteith and Unsworth [11] conducted a theoretical analysis showing

that the SR and by extension other VIs are uniquely related to the amount of incident light reflected and therefore absorbed by a canopy, assuming a low and constant value for soil absorption. Myneni *et al*. [12] showed that NDVI was near-linearly related to the chlorophyll content of single soybean leaves and curvilinearly related to the chlorophyll content of soybean canopies (because surface leaves intercept more light than leaves deeper in the canopy).

Sellers [13] used a canopy radiative transfer model to show that NDVI is near-linearly related to area-averaged net carbon assimilation and plant transpiration, even at different values of f_c and LAI over an area of interest. Hall [14] analyzed the performance of VIs in estimating canopy conductance and transpiration at different scales of measurement over the Konza Prairie in the Great Plains, U.S. Data from ground flux towers were scaled by aerial and satellite imagery to progressively larger landscape units. As in the small-scale studies cited above, they found that NDVI was near-linearly related to canopy carbon assimilation and transpiration and that NDVI values were nearly scale-invariant in going from ground to aerial to satellite measurements. Thus, even in a mixed scene (providing there is no surface water and soil effects are minimal) a VI provides a true measure of area-averaged photosynthetic capacity based on light absorption by chlorophyll, and therefore of processes such as photosynthesis and plant transpiration that are determined by stomatal conduction [13,14]. (Photosynthesis and transpiration are mechanistically linked because carbon dioxide and water molecules enter and exit through stomata on the leaves and stems).

Similar findings have been reported for other VIs. For example, the Enhanced Vegetation Index (EVI) [3] is calculated as:

$$EVI = 2.5 \times (\rho NIR - \rho Red)/(1+ \rho NIR + (6 \times \rho Red - 7.5 \times \rho Blue) \quad (3)$$

where the coefficient "1" accounts for canopy background scattering and the blue and red coefficients, 6 and 7.5, minimize residual aerosol variations. The EVI is more functional on NIR reflectance than on Red absorption, and therefore it does not ”saturate" as rapidly as NDVI in dense vegetation, and it has been shown to be highly correlated with photosynthesis and plant transpiration in a number of studies [3]. The EVI is one of the two VIs available from the MODIS sensors and it is increasingly used in phenological, productivity and evapotranspiration (ET) studies, as documented in **Section 4**. Where soil effects on NDVI are a problem, alternative VIs such as the Soil Adjusted Vegetation Index or the Scaled Difference Vegetation Index can be used [e.g., 15].

3. VIs as Proxies for Other Canopy Attributes

3.1 VIs and LAI

Leaf Area Index (LAI) values are required in many SVAT models to quantify the interception of light by the canopy. The canopy is conceptualized as a series of absorbing layers of leaves, each of which attenuates a fraction of the incident radiation according to the Beer-Lambert Law [16]. In early crop studies, LAIs were used as proxies for canopy light absorption, because fPAR itself was difficult to measure [17,18]. In the 1980s, it became feasible to measure photosynthesis and transpiration in the field on individual leaves enclosed in leaf chambers [19]. SVAT models were developed to scale these leaf-level measurements to whole canopies and stands of plants [16], and these models were then adapted to remote sensing studies [20]. LAIs were needed to scale leaf-level measurements to

complete canopies. VIs or their derivatives are now often used as proxies for LAI in remote-sensing-based SVAT and SEB models, because LAI cannot be measured directly by satellite sensors [21]. In some applications, VIs are combined with look-up tables of vegetation classes to improve the accuracy of LAI predictions [22]. Multiple images taken at different times and over different sensor view angles can be combined to estimate leaf angles and LAI by Bidirectional Reflectance Factor (BRDF) models, which provide structural information about a canopy [23]. However, BRDF models of a canopy can be indeterminate, in that different combinations of LAI and leaf angles can produce similar results [24] (see below). Satellite estimates of LAI can be accurate in some cases [25] but off by a factor of 2 compared to ground estimates in other cases [26]. Furthermore, LAI is difficult to measure on the ground, and optical and leaf-harvesting methods often produce different results [27,28].

LAI is a mathematical construct that does not have a direct relationship to fPAR or processes that depend on fPAR [11]. LAI is usually defined as the one-sided area of leaves in a canopy per unit ground area of canopy cover but non-flat leaves complicate the definition [29]. LAI is related to light interception by a canopy (R_i) by:

$$R_i = R_s(1\text{-}\exp^{-kLAI}) \tag{4}$$

where k is a factor that accounts for leaf angles and other factors that affect absorption of R_s within a canopy [11]. Plants with relatively vertical leaves (erectophiles) typically absorb less light per unit leaf area than plants with relatively horizontal leaves (planophiles). The coefficient k also depends on the arrangement of plants within a stand, because isolated plants receive light from all sides of their canopy whereas a dense stand of plants is only illuminated at the top of the canopy. The fraction of light absorbed by the canopy (fPAR) depends not only on R_i but also on the spectral properties of the leaves. Some leaves have reflective surfaces to minimize heat gain while others absorb nearly all of the incident radiation between 400 and 700 nm. Hence, LAI can be well correlated with NDVI for single plant species grown under uniform conditions [30], but not for mixed canopies, which often occurs in remote sensing studies in which a single pixel can contain several landscape units.

As mentioned, some remote sensing methods to estimate LAI do include estimates of average leaf angle and canopy geometry for particular vegetation types. However, the complexity of using LAI to quantify biophysical processes is illustrated by studies of riparian vegetation on Colorado River in the U.S. [31-36]. Four plant species dominate the riparian corridor, and grow in mixed stands that cannot be easily resolved into individual species even by high-resolution aerial photography and not at all by multiband satellite imagery. Figure 1 shows the leaf structure and light absorption properties of the four species. Arrowweed is an extreme erectophile, with near-vertical leaves often closely appressed to the stem; saltcedar has cylindrical, needle-like leaves, and willow and cottonwood are broad-leafed plants. Field measurements of fPAR, LAI and NDVI show that k in Equation (3) varies from 0.15 for arrowweed to 1.25 for cottonwood, and as a consequence, the LAI required to produce 50% fPAR varies from 4.62 to 0.55. Figure 2 shows LAI, NDVI and ET of these species compared to alfalfa, a common crop plant in irrigation districts along the river. Satellite images typically encompass areas of riparian vegetation as well as agricultural fields. All species had approximately the same LAI, but NDVI values varied by species as predicted by differences in k values, and ET was more closely related to NDVI than to LAI. Clearly, LAI alone is not enough to characterize light-absorption by these species.

Figure 1. Leaf shapes and angles in the canopies, the LAI at which 50% light absorption occurs, and k values for four riparian plant species growing in mixed stands in the Colorado River corridor (from data in [33]).

	LAI @ 50% fPAR	k
AW	4.62	0.15
SC	2.04	0.34
W	1.16	0.60
CW	0.55	1.25

$$fPAR = 1 - e^{-kLAI}$$

Gamon and Qui [37], reviewing remote sensing applications in ecology, pointed out that the use of LAI in SVAT models is partly historical, because photosynthesis and transpiration were formerly measured mainly at the leaf level then scaled up to canopies. This required an estimate of how many layers of leaves were in the canopy and other details of canopy architecture. Today, the most widely accepted measures of plot-level photosynthesis and transpiration are from flux towers (see **Section 4**). These towers unobtrusively measure moisture and carbon fluxes from canopies to the atmosphere over fetches of several thousand square kilometers. Scaling these plot level measurements to larger landscape units by remote sensing does not require knowledge of LAI. Gamon and Qui [37] suggested that the traditional LAI could be replaced by "effective leaf area index" as measured by VIs at the top of the canopy.

3.2 VIs and f_c

Fractional vegetation cover is also required in many SVAT and SEB models that divide the landscape into areas of vegetation and bare soil [6, 38-40]. These models use different methods to estimate carbon and moisture fluxes from vegetation and bare soil and require an estimate of the fraction of the landscape that is vegetated. For example, SEB models of ET use the difference between air temperature and soil temperature (measured by satellite sensors) to estimate bare soil evaporation, but they use the Priestly-Taylor formula for potential ET to estimate transpiration from vegetation [38-40]. Typically, a VI is used to partition the landscape into bare soil and vegetation. NDVI values for a

scene (satellite image) are usually scaled between 0 and 1, representing bare soil (0) and 100% cover (1) to get f_c for a given pixel or area of interest in the scene. In some models, linear scaling is used, and in others the scaling function is non-linear and is adjusted to represent the vegetation type of interest. Some models require both LAI and f_c, and these are often both estimated by VIs [39]. Ground-based information on vegetation type and canopy characteristics can be included to improve the estimates. Sometimes average leaf angles for a particular type of landscape are used to predict both f_c and LAI from VIs [39].

Figure 2. Examples of LAI, NDVI and evapotranspiration (ET) of four riparian species from the Colorado River, with alfalfa for comparison. NDVI, LAI and ET are from natural stands of plants at 100% cover. From data in [31-36]. Alfalfa is from a field along the Colorado River in Blythe, CA, (HayDay Farms, Inc., Nagler *et al*., unpublished data).

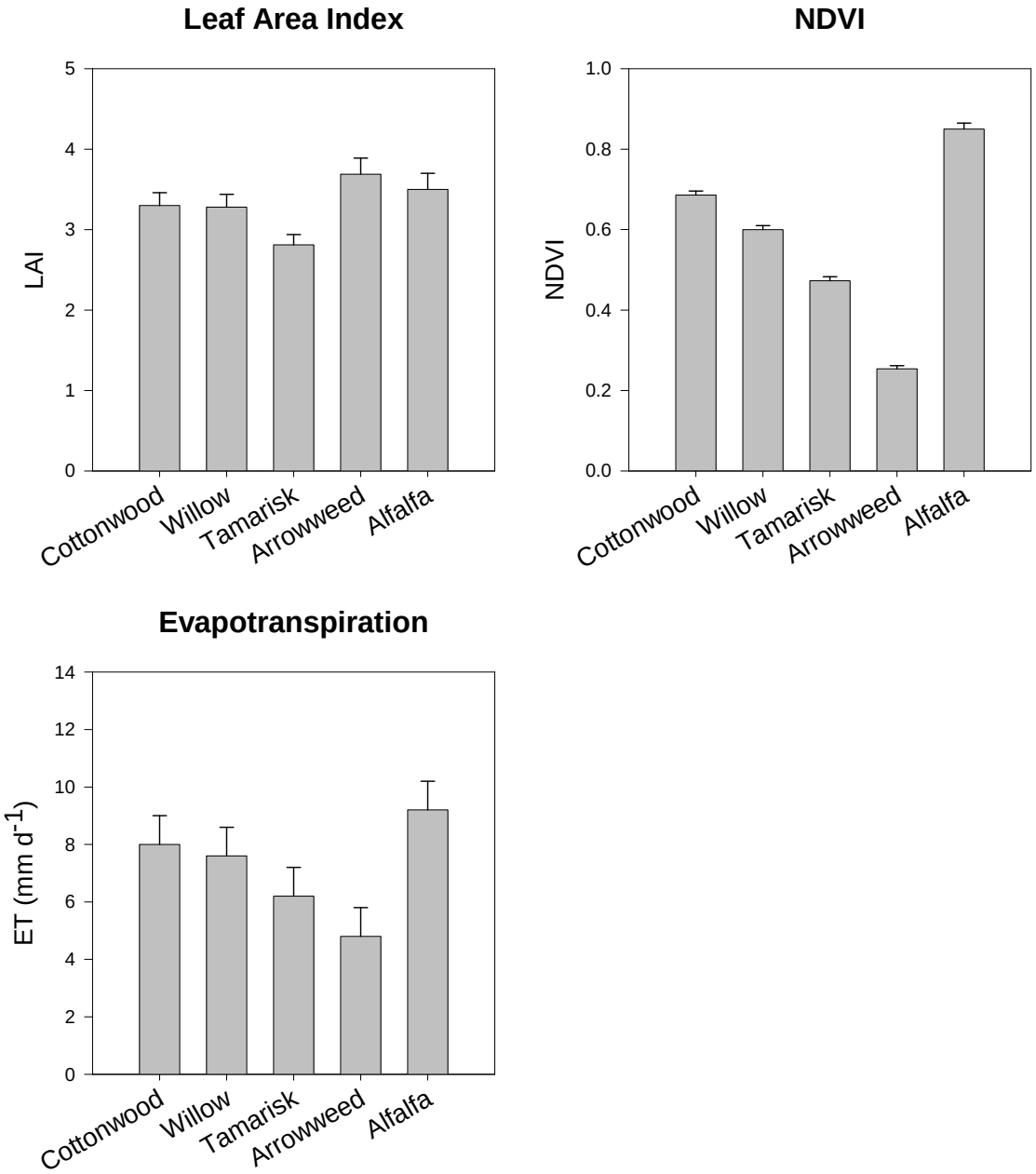

Carlson and Ripley [41] showed that for partially vegetated scenes with LAI in the range of 1-3, VIs were much more closely related to f_c than to LAI of clumped vegetation, and that the relationship between NDVI and f_c was non-linear. They showed that for partially vegetated scenes of uniform vegetation type, VIs were a good measure of f_c. Other studies have also reported strong linear [42] or non-linear [43] relationships between VIs and f_c in a variety of landscape types. However, Figure 2 points out a potential practical problem in using VIs to estimate f_c over mixed scenes. At 100% cover, different plant species may have different VIs due to differences in chlorophyll content and canopy architecture. Figure 3 shows an ETM+ scene containing the same riparian vegetation and agricultural vegetation as in Figure 2 along the Colorado River. Pixels were converted to NDVI values. Fractional cover, determined on high-resolution aerial photographs, was nearly 1.0 for each plant stand highlighted in the figure. However, NDVI values varied among plant types, as expected from Figure 2, and estimates of f_c based on NDVI differed by as much as 40% among species. Alfalfa NDVI was much higher than the riparian species, because fertilized crops tend to have higher chlorophyll content than nitrogen-limited plants in natural ecosystems, due to the large nitrogen cost of chlorophyll and chlorophyll-binding proteins.

Figure 3. NDVI map of a stretch of the Colorado River encompassing agricultural fields and the Havasu National Wildlife Refuge. NDVI values are given for an alfalfa field, a dense stand of saltcedar, a mixed arrowweed-saltcedar stands, and an area dominated by willow trees, all near 100% cover as determined on aerial photographs. From data in [35].

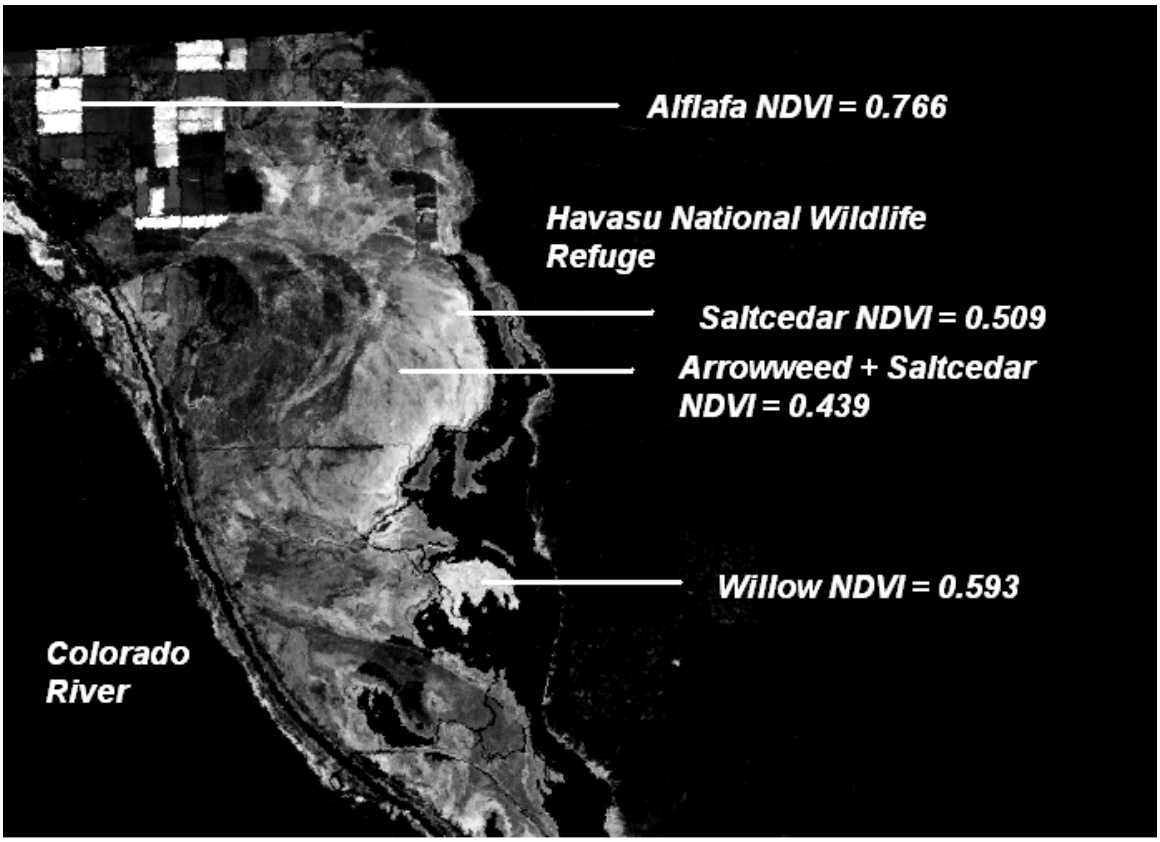

Figure 4 is a scatter plot showing the relationship between NDVI and f_c for riparian vegetation along the Colorado River (agricultural fields excluded). High-resolution (0.3 m) aerial images were

obtained with a DyCam digital camera having Red, Blue and NIR bands. Individual shrubs and bare soil were visible on the images, and a point-intercept method was used to visually determine f_c on 25 images dominated by cottonwood, saltcedar or arrowweed. Then NDVI was determined for each image. Although there was a clear linear relationship between NDVI and f_c (r^2 = 0.81) for the combined images, each species produced a separate regression line corresponding to different NDVI values for full cover shown in Figure 2. Arrowweed, an erectophile, was clearly different from saltcedar and cottonwood. Hence, in mixed scenes, attempts to derive f_c by NDVI would produce bias according to the dominant species present in a given image or pixel. A single satellite pixel often encompasses mixtures of plant types and bare soil.

Figure 4. Relationship between NDVI and fractional vegetation cover for high-resolution aerial DyCam images obtained on the Lower Colorado River. Scenes dominated by arrowweed, cottonwood or saltcedar were selected from a larger collection of images. The regression line of best fit for the combined data are given, as well as lines of best fit for individual species. From data in [33].

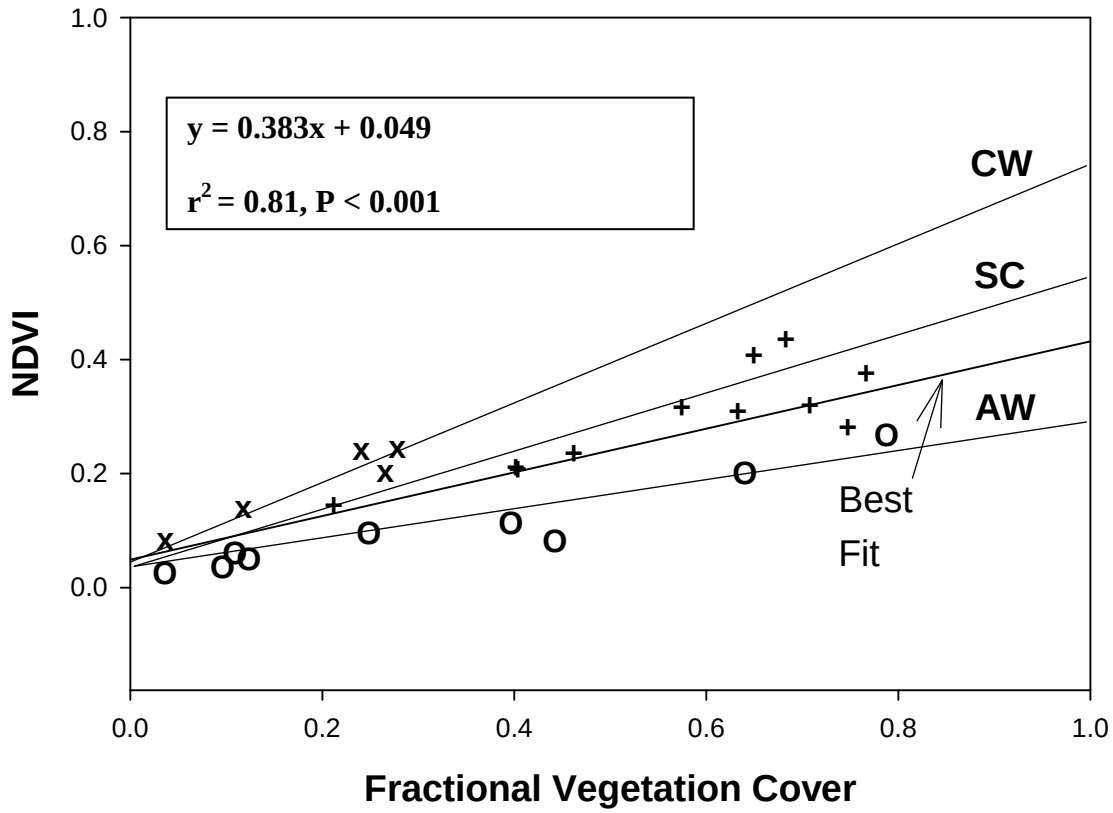

Errors in estimating f_c or LAI by NDVI do not necessarily lead to proportionately large errors in estimating energy fluxes by two-source models. If a pixel is fully vegetated but has low NDVI, it is treated as a partially vegetated pixel in two-source models, with resulting lower estimated latent heat flux than a pixel with high NDVI, a situation close to reality. In a sensitivity analysis of two versions of the two-source Atmosphere-Land Exchange Inverse (ALEXI) ET model, forced variations in LAI of 20% produced variances in estimated sensible heat flux of 10-15% for the so-called "parallel model" compared to 3-7% for the improved "series model", which corrected for clumping of vegetation and its

effect on heat flux from partially vegetated surfaces [43]. Model performance can also be improved by including ground data on LAI and f_c into the model, when such information is available.

However, given the complexities of actual mixed landscapes, estimates of LAI and f_c from VIs and their transformations must be regarded as only approximations for many applications. Furthermore, they are difficult to validate with ground data. Fractional cover can be estimated through aerial photography or on the ground by transect methods [35] but LAI differs among species and changes continuously over a growing season, and actual LAI at validation sites is often poorly known.

3.3 VIs and Roughness Lengths, Emissivity and Albedo

Roughness length (z_0) in meteorology is a measure of the roughness of the surface over which wind is blowing, and it is related to the height and shape of the surface objects that obstruct horizontal flow and convert it to turbulent flow [11]. It is defined as the height above the ground where the logarithmic wind profile goes to zero, and it is approximately 0.1 times the height of the surface elements (e.g., plants). It is a critical term in many SVAT and SEB models because flux rates of mass and energy in and out of canopies are dependent on turbulent flow, and these models require knowledge of z_0. Many remote-sensing SEB and SVAT models use VIs to estimate z_0, either with [e.g. 39,43] or without [e.g. 44] supplementary ground information. For example, the Two Source Time Integrated Model remote sensing model for surface energy fluxes in [39,43] combines NDVI with knowledge of plants heights (when available) to compute f_c and z_0. On the other hand, Surface Energy Balance Algorithm model for surface energy fluxes [44] sometimes assumes a fixed relationship between z_0 and LAI, which is estimated by NDVI.

Unfortunately, the same reservations on using VIs to estimate LAI and f_c apply to roughness lengths. While vegetated surfaces have greater roughness lengths than bare soil, VIs do not adequately capture differences in canopy heights among different vegetation types in mixed scenes [45]. For example, a field of alfalfa 0.5 m tall (e.g., in Figure 3) will have a roughness length of approximately 0.05 m, whereas a saltcedar stand 5 m tall has a roughness length of 0.5 m, 10 times greater; yet, Figure 3 shows that a typical alfalfa field has 50% higher NDVI than saltcedar, which could lead to a large error in estimating turbulent flow by NDVI over a mixed riparian scene containing both agricultural fields and natural vegetation. As mentioned, corrections can be made by supplying plant height data into SEB models but given the complex canopy structure of mixed landscapes, the estimates are approximations.

Emissivity (ε) is the ratio of energy radiated by an object to that radiated by a black body at the same temperature, in which $\varepsilon = 1$for a perfect black body radiator [11]. This relationship is used to measure land surface temperature by satellite sensors in the thermal infrared bands; however, plant canopies and soils are not perfect black body objects ($\varepsilon < 1.0$), and, therefore, estimates of ε are needed to correct satellite-derived land surface temperatures in SEB models that estimate ET by the difference between air temperature and land surface temperature. Albedo is a measure of the fraction of incident radiation diffusely reflected from an object [11], and it is required to calculate net radiation absorbed by the land surface and for other model parameters. Bare soil and vegetation have distinctly different values for emissivity and albedo. Hence, remote sensing models often use transformations of NDVI or other VIs to estimate these parameters. For example, the SEBAL model [44] uses different

transformation of NDVI for fc, albedo, roughness length and ε. Emissivity and albedo are closely correlated with VIs for the vegetated fraction of the landscape, but soils can differ more substantially in the relationship between NDVI, albedo and ε [46-48]. Models that use VIs to estimate these parameters generally first partition the landscape into bare soil and vegetation using VIs, then assign values for emissivity and albedo to each class, e.g. [44]; hence, they are subject to the same types of errors inherent in using VIs to estimate f_c.

4. Combining ground data and VIs to scale biophysical processes over large areas

4.1 Flux Towers and Other Methods to Measure Carbon Assimilation and ET at Plot Scales of Measurement

An alternative to solving complex SVAT and SEB equations with limited remote sensing data is to combine remote sensing measurements with ground data. When ground data are available, remote sensing serves as a scaling tool rather than as a complete physical model. Before the 1990s, carbon and moisture fluxes were difficult to measure at scales relevant to agriculture or ecology. As mentioned, leaf-level measurements were available in the 1980s [19], but it is a daunting task to scale these measurements to whole canopies and larger landscape units. From the 1990s to the present, an increasing number of micrometeorological flux towers have been deployed in agricultural and natural ecosystems around the world [49-51]. These flux towers are now organized into networks such as Euroflux, Ameriflux, MEDEFLUX (the Mediterranean region), AsiaFlux, and OzNet (Australia). In 1997 FLUXNET was formed as a "partnership of partnerships" to compile long-term measurements of carbon dioxide, water vapor and energy flux into high-quality data sets for ecosystems around the world. FLUXNET currently contains 400 towers, and it has the specific goal of validating the remote sensing ecosystem products from the Terra satellite [50].

The existence of flux tower data simplifies the job of scaling plant-related processes over large landscape units. As top-of-canopy measurements, flux towers do not require knowledge of LAI, f_c, or details of canopy architecture to produce results, and the measurement footprint of flux towers at least partially overlaps the pixel size of daily-return satellites (e.g., 250 m for MODIS).

Satellite measurements are spatially continuous at their pixel scale but temporally provide only daily or less frequent snapshots of data, whereas tower-based flux data are temporally continuous at their recording intervals (typically 20-30 minutes), but are essentially point measurements spatially. Hence, combined remote sensing and flux tower data can provide opportunities to upscale the tower data and to constrain the satellite data. Satellites can uniformly sample the entire study area of interest, whereas flux towers seriously under-sample the landscape spatially, but they provide detailed data on fluxes as well as micrometeorological data at frequent intervals over the course of a day.

4.2 What Flux Towers Measure and Sources of Error in Flux Towers

Flux towers measure, among other things, the individual components of the Surface Energy Balance:

$$R_n - G - H - \lambda ET = 0 \quad (5)$$

where λ is the latent heat of evaporation of water; R_n is net radiation flux (R_s minus outgoing short wave and long wave radiation); G is soil heat flux; and H is sensible heat flux to the atmosphere (units are W m^{-2})(flux tower methods are reviewed in [51,52]). Flux towers also measure fluxes of carbon dioxide and other gasses in an out of canopies.

Two types of towers have been widely employed: Bowen Ratio Energy Balance (BREB) and eddy covariance (EC) towers. BREB towers measure gradients of temperature, moisture and carbon dioxide at two points in the turbulent boundary layer over a canopy at (typically) 2 second intervals and data are averaged over 20 minute intervals. Gradients measured over the canopy cannot be used to directly compute fluxes because the transfer coefficients are not known. However, if transfer coefficients for sensible heat and moisture are assumed to be equal their ratio can be calculated (the Bowen ratio) [53]:

$$\beta = \gamma[T_l - T_u]/[e_l - e_u] = H/\lambda ET \quad (6)$$

where γ is the pyschrometric constant, T_l and T_u are upper and lower temperatures and e_l and e_u are lower and upper moisture contents. Then Equations (5) and (6) can be combined to solve for λET:

$$\lambda ET = (R_n - G)/(\beta + 1) \quad (7)$$

BREB towers have net radiometers and soil heat flux plates to measure R_n and G; they can also be used to measure gradients in carbon dioxide and other gasses to determine their fluxes in and out of canopies, assuming their transport coefficients are the same as for moisture and sensible heat.

EC towers are instrumentally more sophisticated than BREB towers [52]. They contain sensitive instruments that measure carbon dioxide, moisture, air temperature and the vertical components of wind speed at a single point over the canopy. Data are collected 20 times per second and are averaged every 30 minutes. Over the longer time scale, the vertical component of wind speed is expected to be zero over a level surface, but at the shorter time scale eddies of air can have a net upward or downward velocity. If, on average, upward eddies have higher moisture content than downward eddies, then a net flux of water out of the canopy is measured over integrated 30 minute data intervals; on the other hand, if downward eddies have higher carbon dioxide content than upward eddies, a net flux of carbon into the canopy is measured. EC towers provide direct measurements of fluxes. Additional instruments measure wind speed, net radiation, soil heat flux and other parameters required in detailed SVAT models and to solve Equation (5).

Flux measurements are subject to several sources of error. They are point measurements, but they require a uniform fetch of vegetation of several thousand square meters (e.g., 50 m x 50 m) around the towers to produce results that are representative of a particular ecosystem, and these conditions are often not perfectly met in natural landscapes. Instrument error and data drop-out introduce errors of about 20% when different towers are intercalibrated at the same site [52]. Furthermore, when EC results are compared to BREB results, EC moisture flux estimates are often 10-30% lower than energy closure (BREB) results. EC results are often increased to account for this “closure error” [54], but the best way to achieve closure, and the cause of the closure error, are still unclear [51,52].

Flux towers measure net ecosystem rates of carbon dioxide and moisture fluxes in and out of canopies. Net carbon fluxes are due to net uptake by plants in photosynthesis during the day, release of carbon dioxide by plants at night, and by soil respiration and litter decomposition. Net moisture fluxes

are due to bare soil evaporation plus plant transpiration minus precipitation and condensation. Top-of canopy flux towers can be combined with under-canopy measurements to calculate soil and understory respiration [55] and plant transpiration can be measured with sap flow sensors [56], which measure the flow of water through plant stems. Natural isotopes of oxygen and hydrogen can also be used to distinguish between evaporation and transpiration in ET [57]. Hence, the individual components of carbon and moisture fluxes can be measured at tower stations.

Flux tower and sap flow data can also test cause-and-effect relationships between meteorological and soil variables and plant performance that can inform ecophysiological studies. For example, it is possible to invert the Penman-Monteith equation for ET, to obtain frequent estimates of stomatal conductance (or resistance) in response to stress factors under natural conditions over the course of hours, days, weeks, seasons and years [58]. An example using three of the plant species shown in Figures 1-4 is in Figure 5. Sap flow was measured in plants for seven days under unstressed conditions and correlated with micrometeorological data to produce a stomatal resistance model for each species [36]. Then the plants were subjected to salt stress and dry-down, and measured stomatal resistance was compared to modeled values over three subsequent days. All three species had similar patterns of transpiration and stomatal resistance under unstressed conditions, but the two mesic trees, cottonwood and willow, showed increased stomatal resistance in response to stress, whereas saltcedar, which is drought- and salt-tolerant, did not increase its stomatal resistance. The type of experiments illustrated in [36] and [58] were formerly only possible over short intervals on individual leaves enclosed in leaf chambers, but they now can be performed unobtrusively on whole plants [36] and mixed stands of plants [58].

4.3 Examples of Combining VIs and Flux Tower Data to Estimate Carbon Fluxes

Measuring landscape-level carbon fluxes is essential in global change studies [e.g., 50]. Gross Primary Production (GPP) is defined as the amount of CO_2 fixed in photosynthesis, while Net Primary Production (NPP) is defined as GPP minus plant respiration [59]:

$$NPP = GPP - (R_{leaves} + R_{roots} + R_{woody\ tissues}) \quad (8)$$

GPP can be estimated by satellite data based on the linear relationship between fPAR and VIs, for example NDVI:

$$GPP = LUE \times fPAR \times PAR = ca.\ LUE \times NDVI \times PAR \quad (9)$$

where LUE is Light Use Efficiency, the PAR conversion efficiency [59]. LUE values vary widely with vegetation type and environmental conditions. Currently, LUE and the respiration terms in (8) are estimated by modeling, using assumed values of parameters for broad biome types. For example, MODIS products include a combined, NDVI-based, LAI – fPAR term that is combined with meteorological variables and look-up tables of specific leaf area and respiration values for general biome types (evergreen needleleaf forest, deciduous broadleaf forest, shrubland, savanna, grassland, and cropland) to estimate GPP and NPP [59-61].

These models can be validated and improved by combining them with flux tower data [62-64]. Flux towers can estimate GPP and NPP separately by comparing daytime NPP with nighttime respiration

and by other techniques, and LUE can also be calculated directly from canopy carbon fluxes divided by net radiation [50,51].

Time-series VIs and tower data have been successfully combined in a number of recent studies of ecosystem carbon exchange. Wylie et al. [65] showed that NDVI from AVHRR could be calibrated with BREB flux tower data to provide accurate 14-day estimates of daytime and nighttime carbon exchange from a sagebrush-steppe ecosystem in Idaho, and suggested that portable flux towers could be deployed to increase the spatial coverage of tower data. Using a hand-held radiometer in grazed and ungrazed prairie sites, Frank and Karn [25] found strong linear relationships between NDVI and carbon dioxide and moisture fluxes measured at towers, and strong but non-linear relationships between NDVI and LAI and standing biomass. They concluded that NDVI has the potential for predicting carbon and water fluxes in semiarid grasslands and shrublands.

Huete *et al*. [66] found a consistent linear relationship between seasonal MODIS EVI and tower calibrated GPP in intact rainforests and rainforest land converted to pasture and agriculture in the Amazon. In relation to tower measured GPP, the MODIS EVI did not saturate in such high biomass tropical rainforests. Saleska *et al*. [67] used this relationship to show that, contrary to ecosystem models of the Amazon, the forests are greener in the dry season than in the wet season, and a period of drought in 2005 actually stimulated carbon fixation rather than inhibiting it. Plants used water stored in the soil profile to support growth, and took advantage of higher radiation levels in the dry periods. Huete *et al*. [68] extended these studies to three distinct Monsoon Asia tropical forests and found similar MODIS EVI and tower GPP linear relationships across the multiple sites, potentially offering promising opportunities for regional scaling of carbon fluxes across the heterogeneous canopies of Southeast Asia.

Sims *et al*. [69] and Rahman *et al*. [70] also found a strong relationship between tower GPP and MODIS EVI across a wide range of biome types and concluded that EVI can be used to estimate GPP directly, without direct consideration of LUE required in many SVAT models. This simplifies the estimation of GPP, as LUE is difficult to determine by direct measurement. Yuan *et al*. [71] used NDVI to estimate fPAR, and found that a simple LUE model moderated by temperature and soil moisture could predict daily gross primary productivity from 28 EC flux towers over forests, grasslands and savannas with coefficients of determination (r^2) of 0.77 - 0.85.

Further work is needed on how best to integrate satellite data into ecosystem production efficiency models. Attempts to improve upon the satellite EVI and tower GPP relationships through the use of PAR and fPAR variables have been generally unsuccessful [72,73] in part due to the weaker correlation of fPAR with satellite NDVI compared to EVI. There is a need to better separate canopy absorbed PAR into the photosynthetically-active (chlorophyll) and non-active (senesced vegetation, woody material) components and better understand the seasonal hysteresis observed in satellite greenness relationships with tower measured fPAR data [73]. Xiao *et al.* [72] distinguished between the photosynthetically-active and non-photosynthetically active components of canopy absorbed radiation, and reported the EVI to be more closely related to the chlorophyll component of fPAR, while NDVI was more closely correlated with total canopy fPAR. Unlike NDVI, EVI incorporates both Blue and Red bands in its formulation, and chlorophyll absorbs strongly in both the Blue and Red bands. Grace et al. [74] proposed combining VIs with remotely-sensed chlorophyll florescence, an indicator of plant stress, to derive LUE from remote sensing data alone.

4.4 Examples of VIs and Flux Tower Data to Estimate ET

Remote sensing approaches to estimating ET have historically used measurements of land surface temperature (LST) from Thermal Infrared (TIR) sensors as the key satellite measurement [6, 38, 39, 40, 43, 44]. These methods were developed starting in the 1970s and continue to dominate ET studies today. They typically use the difference between air temperature (measured on the ground) and LST (measured by satellites) to estimate sensible heat flux from the land surface. Then they obtain estimates of R_n and G from ground or remote sensing data (typically from VIs) and compute ET, expressed as the latent heat of evaporation, as a residual in the surface energy balance (Equation 4). These methods present a number of difficulties due in part to the lack of 1:1 correspondence between the LST measured by satellite and the so-called "aerodynamic surface temperature" required to calculate H [6, 38], and a number of methods have been devised to surmount this problem using context within the imagery, e.g. [38, 39, 44, 75].

Recent studies have combined flux tower measurements of ET with time-series VIs to accurately scale ET over larger landscape units without the use of LST. They take advantage of the strong correlation between ET and VIs observed in numerous studies. Table 1 gives correlation coefficients between ET and MODIS EVI or NDVI at 11 tower sites in the southwestern U.S. The sites included nine riparian sites with different types of vegetation [34], plus one upland shrub site and one upland grass site [76]. Towers included both BREB and EC types. ET values from towers were compiled in 16-day intervals over multiple years and correlated with 16-day composite MODIS VI values. The correlation analysis used the single MODIS pixel encompassing the tower location at each site.

EVI was strongly correlated with ET at all tower sites, and correlation coefficients were higher for EVI than NDVI at all sites. At the riparian sites, EVI combined with maximum daily air temperature (T_a) across all sites produced a simple model that predicted ET with $r^2 = 0.79$, leaving only 21% of the variance in ET unexplained. At the two semiarid upland sites, EVI plus precipitation produced a model with an $r^2 = 0.76$, even though the sites were only 20-25% vegetated. ET is dominated by T from vegetation even in dry ecosystems, and VIs (especially the EVI) clearly have great potential for scaling point measurements of ET over large areas.

Nagler *et al*. [34] used the EVI-T_a relationship to produce tower-validated estimates of ET for the major vegetation types on western U.S. rivers and reported that the exotic species saltcedar, thought to be a heavy water user, actually had low to moderate rates of ET compared to native species. Cleugh *et al*. [77] combined MODIS NDVI and surface meteorology data to estimate ET in two different Australian ecosystems, and reported $r^2 = 0.74$ between remote sensing and tower measurements, demonstrating the validity of the method over regional scales of measurement. Mu *et al*. [78] used MODIS EVI and meteorological data to predict ET at the continental scale, and produced $r^2 = 0.76$ when estimates were compared to ET measured at 19 Ameriflux towers. They extended their model to the global scale, and concluded that MODIS EVI and ground meteorological data can be used to provide critical information on the regional and global water cycle resulting from environmental changes. Yang *et al*. [79] combined MODIS EVI meteorological data in a Machine Learning Program to predict ET at 19 towers sites with $r^2 = 0.75$ for the conterminous U.S., and Wang *et al.* [80] combined MODIS EVI, T_a and surface net radiation to predict ET in the Southern Great Plains of the U.S. with $r^2 = 0.83$ compared to flux tower values. The accuracy of the ET predictions in each case is

within the error and uncertainty range inherent in the flux tower measurements of ET. In the special case of phreatophytic vegetation rooted into deep soil water in arid zones, Groeneveld *et al*. [81] found that a single mid-summer, high-resolution NDVI image calibrated against potential ET could predict actual annual ET determined by flux towers with acceptable accuracy across a wide range of vegetation types.

Table 1. Correlation coefficients between evapotranspiration measured at moisture flux towers and MODIS vegetation indices and relevant meteorological data in the southwestern U.S. T_a is maximum daily temperature and P is precipitation. Correlation coefficients for combined variables are for the multiple linear regression equation of best fit for combined riparian (EVI + T_a) or upland (EVI + P) sites. From data in [31,34,76].

Tower Site	Vegetation	EVI	NDVI	T_a	P	EVI + T_a	EVI + P
Riparian							
San Pedro 1	Mesquite	0.87	0.83	0.77	-	0.88	-
San Pedro 2	Mesquite	0.86	0.82	0.77	-	0.90	-
San Pedro 3	Sacaton	0.94	0.82	0.77	-	0.97	-
Rio Grande 1	Saltcedar	0.83	0.68	0.84	-	0.88	-
Rio Grande 2	Saltcedar	0.84	0.52	0.82	-	0.89	-
Rio Grande 3	Cottonwood	0.84	0.74	0.86	-	0.90	-
Rio Grande 4	Cottonwood	0.82	0.77	0.89	-	0.89	-
Colorado 1	Saltcedar	0.83	0.64	0.92	-	0.92	-
Colorado 2	Arrowweed	0.64	0.50	0.76	-	0.79	-
Upland							
Grassland	Grama	0.82	0.80	-	0.66	-	0.84
Shrubland	Mixed	0.87	0.78	-	0.72	-	0.90
Mean		0.83	0.72	0.82	0.69	0.89	0.87

VI methods for ET are valuable monitoring tools but they cannot be used as early indicators of plant stress, important in irrigation scheduling and other water management tasks. However, VIs can be combined with satellite-derived LSTs to provide estimates of ET, soil moisture conditions and land use changes, as in the “triangle method” where pixel values of NDVI and LST are plotted against each other to produce a response surface of vegetation density and surface temperature [75].

5. Reformulating SVAT models to accommodate new data sources

Shuttleworth [49] described the history of evaporation research over the past 30 years as a series of loosely-linked conceptual and technical advances leading to the present state of the science. Carbon flux studies parallel that history [16,37]. Gamon and Qui [37] pointed to the historical connection between SVAT parameters and what could be measured at the time the models were developed. Historically, SVAT and SEB models have taken a "bottom-up" approach, attempting to scale leaf level measurements to whole canopies and stands of plants [16]. For example, the Penman-Monteith

equation [11] for ET treats the canopy as a series of resistances, starting with individual stomata at the leaf level then proceeding to the canopy level, where the atmospheric resistance term is applied.

Figure 5. Stomatal resistance of cottonwood, willow and saltcedar plants under stressed and unstressed conditions. Clusters of plants (6 per species) were grown outdoors in Tucson, Arizona. Sap flow sensors measured plant transpiration over an eight day period in summer, and micrometeorological data were used to model the diurnal course stomatal resistance for each species based on potential ET. Plants were then subjected to drought or salt stress (3 per treatment) for the final 3 days of the measurement period. Stomatal resistance was calculated based on sap flow measurements at three time points in the mid-day period, and plotted against unstressed stomatal resistance calculated from meteorological data. Plants are combined across replicates and stress treatments in the plot. From data in [36].

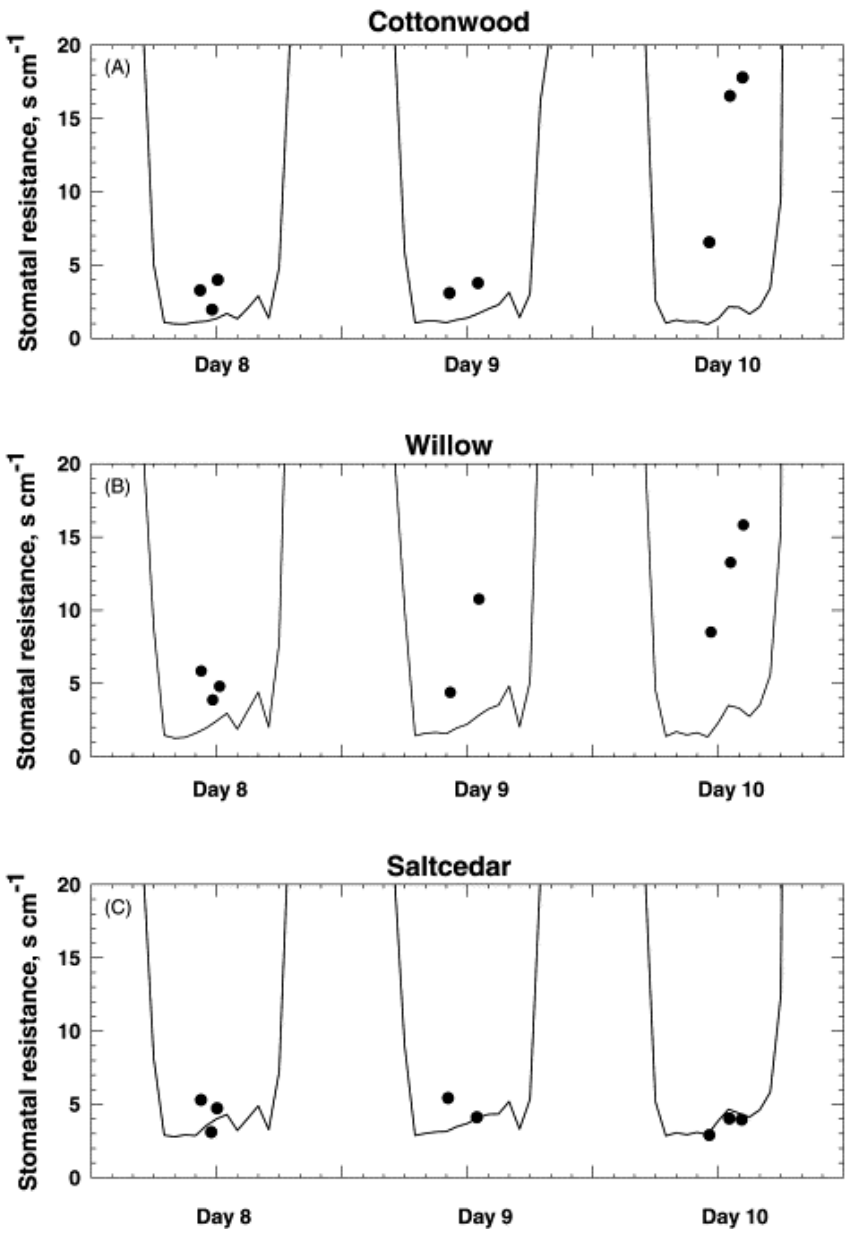

Carbon flux models usually start at the leaf level as well, sometimes assuming Michaelis-Menton kinetics for carbon fixation as functions of light intensity and carbon dioxide concentration as starting points, then using radiation transfer models to scale light intensity and photosynthesis over the layers of leaves in the canopy [16]. These models were developed when leaf-level measurements of photosynthesis and stomatal conductance were becoming feasible.

The bottom up approach has encountered some problems in remote sensing applications, however. First is the complexity of actual plant canopies, especially in mixed stands of plants, compared to what can be determined from remote sensing measurements. Second is the problem of equifinality, the tendency of models with different levels of complexity and different starting assumptions to produce similar results [82]. This has also been called the problem of underdetermination, when a single data set can be used to support multiple competing hypotheses. Models that use remote sensing data are prone to this type of error because the same VIs, or transformations of VIs, are often used to estimate more than one model parameter, introducing co-linearity, and because the ground data by which they are calibrated or validated have errors or uncertainties on the order of 20-30%. The traditional approach to resolving problems of underdetermination is to prefer the simpler model or hypothesis over the more complex (Occam's Razor) [83], although this is a philosophical rather than a scientific principle.

With the advent of flux towers and moderate resolution, daily return satellite imagery, a different approach has become feasible. Top-of-canopy measurements of fluxes can be scaled to larger landscape units using simple models developed from ground data and VIs. Tower data can then be used to invert SVAT models to test hypotheses about the controls on photosynthesis, growth and water consumption at the plot scale, and changes in foliage density over time revealed by satellite sensors can be used to scale these findings to the ecosystem or biome scales of measurement. Plant stress detected at the towers is detectable by satellites first as an anomaly in VI:surface temperature plots [75] and latter as a drop in VI as plants adjust their foliage density to match the limiting conditions [4].

A recent successful example of the combined approach was the use of flux tower and MODIS EVI data in the Amazon to show that ET and GPP increased, rather than decreased, in response to seasonal or interannual dry periods, contrary to model results [66,67].Those papers concluded that more observational data and less reliance on models could lead to more accurate predictions of climate change effects on global ecosystems.

To take advantage of the new tools, it might be necessary to reformulate traditional SVAT and SEB models that use VIs as proxies for LAI, f_c, and other canopy attributes that are only moderately well predicted by remote sensing measurements, as recommended in [37]. One approach is to use so-called Big Leaf models of carbon fixation and stomatal conductance [49]. These models, first suggested by Monteith in 1965 [cited in 49], treat the canopy and associated unvegetated areas as a single surface, and use average leaf and surface properties as scalars. Big Leaf models are especially well suited to satellite sensors and flux towers that provide top of the canopy measurements. Big Leaf models frequently perform as well as multilayer SVAT models in actual applications, e.g. [84]. Although they oversimplify actual canopies, they can produce accurate results when calibrated with flux tower or other ground data [16]. Current Big Leaf models still require an estimate of LAI, because they take average leaf properties then scale them over the canopy by multiplying by LAI [20,49]. However, in principal LAI could be replaced by a VI in these models [37].

6. Conclusions

VIs and their transformations and derivatives are extremely useful tools in monitoring processes related to fPAR absorbed by vegetation. These include processes related to photosynthesis at the canopy or ecosystem scale (phenology, primary productivity, net carbon fixation, gross primary productivity), and processes related to plant transpiration (ET, rainfall use efficiency, groundwater withdrawal). VIs are measures of green foliage density, and they must be combined with ground data or appropriately calibrated models to produce accurate information about these processes. VIs represent composite properties of f_c, LAI, and canopy architecture and they are only moderately useful in predicting individual canopy properties required in SVAT and SEB models. Therefore, remote sensing methods for estimating ecosystem variables should be formulated in ways that take advantage of their strengths and minimize their weaknesses. Remote sensing applications are perhaps strongest when they are used as scaling tools for observational ground data rather than as detailed physical models of the landscape.

References

1. Pettorelli, N.; Vik, J.; Mysterud, A.; Gaillard, J.; Tucker, C.; Stenseth, N. Using the satellite-derived NDVI to assess ecological responses to environmental change. *Trends in Ecology and Evolution* **2005**, *20*, 503-510.
2. Kerr, J.; Ostrovsky,M. From space to species: ecological applications for remote sensing. *Trends in Ecology and Evolution* **2003**, *18*, 299-305.
3. Huete, A.; Didan, K., van Leeuwen, W., Miura, T.; Glenn, E. MODIS vegetation indices. *In Land Remote Sensing and Global Environmental Change: NASA's Earth Observing System and the Science of ASTER and MODIS* **2008**, in press.
4. Field, C. Ecological scaling of carbon gain to stress and resource availability. In H. Mooney, W. Winner, & E. Pell (eds.), *Response of Plants to Multiple Stresses* **1991**, London, Academic Press, pp. 35-66.
5. Ninemets, U. Photosynthesis and resource distribution through plant canopies. *Plant, Cell and Environment* **2007,** *30*, 1052-1071.
6. Glenn, E.; Huete, A.; Nagler, P.; Hirschboeck, K.; Brown, P. Integrating remote sensing and ground methods to estimate evapotranspiration. *Critical Reviews in Plant Sciences* **2007**, *26*, 139-168.
7. Jordan, C. Derivation of leaf-area index from quality of light on the forest floor. *Ecology* **1969**, *50*, 663-666.
8. Rouse, J.; Hass, R.; Schell, J.; Deering, D. Monitoring vegetation systems in the great plains with ERTS. *Third ERTS Symposium* **1973**, NASA, SP-351 I, 309-317.
9. Tucker, C.; Townshend, J.; Goff, T. African land cover classification using satellite data. *Science* **1985**, *227*, 229-235.
10. Tucker, C. Red and photographic infrared linear combinations for monitoring vegetation. *Remote Sensing of Environment* **1979**, *8*, 127-150.

11. Monteith, J.; Unsworth, M. *Principles of Environmental Physics, 2nd. Edition*. **1990**, Edward Arnold, London.
12. Myneni, R,; Hall, F., Seller, P.; Marshak, A. The interpretation of spectral vegetation indexes. *IEEE Transactions on Geoscience and Remote Sensing* **1995**, *33*, 481-
13. Sellers, P. Canopy reflectance, photosynthesis and transpiration. *International Journal of Remote Sensing* **1985**, *6*, 1335-1372.
14. Hall, F. Satellite remote sensing of surface energy balance: success, failures and unresolved issues in FIEF. *Journal of Geophysics Research* **1992**, *97*, 19061-19090.
15. Jiang, Z.; Huete, A.; Chen, J.; Chen, Y.; Li, J.; Yan, G.; Zhang, X. Analysis of NDVI and scaled difference vegetation index retrievals of vegetation fraction. *Remote Sensing of Environment* **2006**, *101*, 366-378.
16. Beyschlag, W.; Ryel, R. Canopy photosynthesis modeling. In *Functional Plant Ecology*. Pugnaire, F.; Valladares, F., (eds.); Taylor & Francis Group: Boca Raton, FL, **2007**; pp. 627-654.
17. Harper, P. Optimum leaf area index in the potato crop. *Nature* **1963**, *4770*, 917-918.
18. Stern, W.; Donald, C. Relationship of radiation, leaf area index and crop growth rate. *Nature* **1961**, *4764*, 597-598.
19. Pearcy, R.; Schulze, E.; Zimmermann, R. Measurement of transpiration and leaf conductance. In: *Plant Physiological Ecology*; Pearcy, R, Ehleringer, J., Mooney, H., Rundel, P., (Eds.); Chapman & Hall: London, **1991**; pp. 137–160.
20. Sellers, P.; Randall, D.; Collatz, G.; Berry, J.; Field, C.; Dazlich, D.; Zhang, C.; Collelo, G.; Bounoua, L. A revised land surface parameterization (SiB2) for atmospheric GCMs. 1. Model formulation. *Journal of Climate* **1996**, *9*, 676-705.
21. Liang, S. Recent developments in estimating land surface biogeophysical variables from optical remote sensing. *Progress in Physical Geography* **2007**, *31*, 501-516.
22. Wang, Y.; Woodcock, C.; Buermann, W.; Stenberg, P.; Voipio, P.; Smolander, H.; Hame, T.; Yuhong, T.; Hu, J.; Knyazikhin, Y.; Myneni, R. Evaluation of the MODIS LAI algorithm at a coniferous forest site in Finland. *Remote Sensing of Environment* **2004**, *91*, 114-127.
23. Roberts, G. A review of the application of BRDF models to infer land cover parameters at regional and global scales. *Progress in Physical Geography* **2001**, *25*, 483-511.
24. Widowski, J.; Pinty, B.; Lavergne, T.; Verstraete, M.; Gobron, N. Using 1-D models to interpret the reflectance anisotropy of 3-D canopy targets: Issues and caveats. *IEEE Transactions on Geoscience and Remote Sensing* **2005**, *43*, 2008-2017.
25. Frank, A.; Karn, J. Vegetation indices, CO_2 flux, and biomass for Northern Plains grasslands. *Journal of Range Management* **2003**, *56*, 382-387.
26. Leuning, R.; Cleugh, H.; Zegelin, S.; Hughes, D. Carbon and water fluxes over a temperate Eucalyptus forest and a tropical wet/dry savanna in Australia: measurements and comparison with MODIS remote sensing estimates. *Agricultural and Forest Meteorology* **2005**, *129*, 151-173.
27. Asner, G.; Scurlock, J.; Hicke, J. Global synthesis of leaf area index observations: implications for ecological and remote sensing studies. *Global Ecology and Biogeography* **2003**, *122*, 191-205.

28. Breda, N. Ground-based measurements of leaf area index: a review of methods, instruments and current controversies. *Journal of Experimental Botany* **2003**, *54*, 2403-2417.
29. Chen, J.; Black, T. Defining leaf area index for non-flat leaves. *Plant, Cell & Environment* **1992**, *15*, 21-29.
30. Asrar, G.; Kanemasu, E.; Yoshida, M. Estimates of leaf area index from spectral reflectance of wheat under different cultural practices and solar angles. *Remote Sensing of Environment* **1985**, *17*, 1-11.
31. Nagler, P.; Cleverly, J.; Lampkin, D.; Glenn, E.; Huete, A.; Wan, Z. Predicting riparian evapotranspiration from MODIS vegetation indices and meteorological data. *Remote Sensing of Environment* **2005**, *94*, 17-30.
32. Nagler, P.; Glenn, E.; Huete, A. Assessment of vegetation indices for riparian vegetation in the Colorado River delta, Mexico. *Journal of Arid Environments* **2001**, *49*, 91-110.
33. Nagler, P.; Glenn, E.; Thompson, T.; Huete, A. Leaf area index and Normalized Difference Vegetation Index as predictors of canopy characteristics and light interception by riparian species on the Lower Colorado River. *Agricultural and Forest Meteorology* **2004**, *116*, 103-112.
34. Nagler, P.; Scott, R.; Westenberg, C.; Cleverly, J.; Glenn, E.; Huete, A. Evapotranspiration on western U.S. rivers estimated using the Enhanced Vegetation Index from MODIS and data from eddy covariance and Bowen ratio flux towers. *Remote Sensing of Environment* **2005**, *97*, 337-351.
35. Nagler, P.; Glenn, E.; Hursh, K.; Curtis, C.; Huete, A. Vegetation mapping for change detection on an arid-zone river. *Environmental Monitoring and Assessment* **2005**, *109*, 255-274.
36. Nagler, P.; Glenn, E.; Thompson, T. Comparison of transpiration rates among saltcedar, cottonwood and willow trees by sap flow and canopy temperature methods *Agricultural and Forest Meteorology* **2003**, *116*, 73-89.
37. Gamon, J.; Qui, H. Ecological applications of remote sensing at multiple scales. In F. Pugmaore and F. Valladares (eds.), *Handbook of Function Plant Ecology* **2007**, Taylor and Francis Group, Boca Raton, FL, pp. 655-684.
38. Kustas, W.; Norman, J. Use of remote sensing for evapotranspiration monitoring over land surfaces. *Hydrological Sciences Journal - Journal des Sciences Hydrologiques* **1996**, *41*, 495-516.
39. Anderson, M. A two-source time-integrated model for estimating surface fluxes using thermal infrared remote sensing. *Remote Sensing of Environment* **1997**, *60*, 195-216.
40. Timmerman, W.; Kustas, W.; Anderson, M.; French, A. An intercomparison of the Surface Energy Balance Algorithm for Land (SEBAL) and the Two-Source Energy Balance (TSEB) modeling schemes. *Remote Sensing of Environment* **2007**, *108*, 369-384.
41. Carlson, T.; Ripley, D. On the relationship between fractional vegetation cover, leaf area index, and NDVI. *Remote Sensing of Environment*, **1997**, *62*, 241-252.
42. Ormsby, J.; Choudry, B.; Owe, M. Vegetation spatial variability and its effect on vegetation indexes. *International Journal of Remote Sensing* **1987**, *8*, 1301-1306.
43. Li, F.; Kustas, W.; Preuger, J.; Neale, C.; Jackson, T. Utility of remote sensing-based two-source balance model under low- and high-vegetation cover conditions. *Journal of Hydrometeorology* **2005**, *6*, 878-891.

44. Bastiaanssen, W.; Menentia,M.; Feddes,R.; Holstag, A. A remote sensing surface energy balance algorithm for Land (SEBAL), Part I, Formulation. *Journal of Hydrology* **1998**, *212-213*, 198-212.
45. Lagouarde, J.; Jacob, J.; Gu, X.; Olioso, A.; Bonnefond, J.; Kerr, Y.; McAneney, K.; Irvine, M. Spatialization of sensible heat flux over a heterogeneous landscape. *Agronomie* **2002**, *22*, 627-633.
46. Jimenez-Munoz, J.; Sobrino, J.; Gillespie, A.; Sabol, D.; Gustafson, W. Improved land surface emissivities over agricultural areas using ASTER NDVI. *Remote Sensing of Environment* **2006**, *103*, 474-487.
47. Momeni, M.; Saradjian, M. Evaluating NDVI-based emissivities of MODIS bands 31 and 32 using emissivities derived by Day/Night LST algorithm. *Remote Sensing of Environment* **2007**, *106*, 190-198.
48. Wittich, K.; Kraft, M. The normalized difference vegetation index obtained from agrometeorological standard radiation sensors: a comparison with ground-based multiband spectroradiometer measurements during the phenological development of an oat canopy. *International Journal of Biometeorology* **2008**, *52*, 167-177.
49. Shuttleworth, W. Putting the 'vap' in evaporation. *Hydrology & Earth System Sciences* **2007**, *11*, 210-244.
50. Baldocchi, D.; Falge, E.; Gu, L., Olson, R.; Hollinger, D.; Running, S.; Anthone, P.; Berhofer, C.; Davis, K.; Evans, R.; Fuentes, J.; Goldstein, A.; Katul, G.; Law, B.; Lee, X.; Malhi, Y.; Meyers, T.; Munger, W.; Oechel, W.; Pilegaard, K.; Schmid, H.; Valentini, R.; Verma, S.; Vesala, T.; Wilson, K.; Wofsy, S. Fluxnet: a new tool to study the temporal and spatial variability of ecosystem-scale carbon dioxide, water vapor, and energy flux densities. *Bulletin of the American Meteorological Society* **2001**, *82*, 2415-2434.
51. Baldocchi, D. Assessing the eddy covariance technique for evaluating carbon dioxide exchange rates of ecosystems: past, present and future. *Global Change Biology* 2003, **9**, 479-492.
52. Rana, G.; Katerji, N. Measurement and estimation of actual evapotranspiration in the field under Mediterranean climate: a review. *European Journal of Agronomy* **2000**, *13*, 125-153.
53. Bowen, I. The ratio of heat losses by conduction and by evaporation from any water surface. *Physical Review* **1926**, *27*, 779-787.
54. Twine, T.; Kustas, W.; Norman, J.; Cook, D.; Houser, P.; Meyers, T.; Prueger, J.; Starks, P.; Weslely, M. Correcting eddy-covariance flux underestimates over a grassland. *Agricultural and Forest Meteorology* **2000**, *103*, 279-300.
55. Misson, L.; Baldocchi, D., Black, T., Banken, P.; Falk, M.; Granier, A.; Irvine, M.; Jarosz, N.; Lamaud, E.; Launiainen, S.; McKay, M.; Paw, K.; Vesala, T.; Vickers, D.; Wilson, K.; Goldstein, A. Partitioning forest carbon fluxes with overstory and understory eddy-covariance measurements: A synthesis based on FLUXNET data. *Agricultural and Forest Meteorology* **2007**, 144, 14-31.
56. Scott, R.; Huxman, T.; Cable, W.; Emmerich, W. Partitioning of evapotranspiration and its relation to carbon dioxide exchange in a Chihuahuan Desert shrubland. *Hydrological Processes* **2006**, *20*, 3227-3243.

57. Yepez, E.; Williams, D.; Scott, R., Lin, G. Partitioning overstory and understory evapotranspiration in a semiarid savanna woodland from the isotopic composition of water vapor. *Agricultural and Forest Meteorology* **2003**, *119*, 53-68.
58. Scott, R.; Edwards, E.; Shuttleworth, W.; Huxman, T.; Watts, C.; Goodrich, D. Interannual and seasonal variation in fluxes of water and carbon dioxide from a riparian woodland ecosystem. *Agricultural and Forest Meteorology* **2004**, *122*, 65-84.
59. Running, S.; Nemani, R.; Heinsch, F.; Zhao, M.; Reeves, M.; Hashimoto, H. A continuous satellite-derived measure of global primary production. *Bioscience* **2004**, *54*, 547-560.
60. Potter, C.; Klooster, S.; Huete, A.; Genovese, V. Terrestrial carbon sinks for the United States predicted from MODIS satellite data and ecosystem modeling. *Earth Interactions* **2007**, *11*, Art. No. 13.
61. Zhao, M.; Heinsch, R.; Nemani, R.; Running, W. Improvements of the MODIS terrestrial gross and net primary production global data set. *Remote Sensing of Environment* **2005**, *95*, 164-176.
62. Yuan. W.; Liu, S.; Zhou, G.; Zhou, G.; Tieszen, L.; Baldocchi, D.; Bernhofer, C.; Gholz, H.; Goldstein, A.; Goulden, M.; Hollinger, D.; Hu, Y.; Law, B.; Stoy, P.; Vesala, T.; Wofsy, S. Deriving a light use efficiency model from eddy covariance flux data for predicting gross primary production across biomes. *Agricultural and Forest Meteorology* **2007**, *143*, 189-207.
63. Owen, K.; Tenhunen, J.; Reichstein, M.; Wang, Q.; Falge, E.; Geyer, R.; Xiao, X.; Stoy, P.; Ammann, C.; Arain, A.;Aubiinet, M.; Aurela, M.; Bernhofer, C.; Chojnicki, B.; Granier, A.; Gruenwald, T.; Hollinger, D.; Knohl, A.; Kutsch, W., Lohila, A.; Meyers, T.; Moors, E.; Moureaux, C.; Pilegaard, K., Saigusa, N.; Verma, S.; Vesala, T.; Vogel, C. Linking flux network measurements to continental scale simulations: ecosystem carbon dioxide exchange capacity under non-water-stressed conditions. *Global Change Biology* **2007**, *13*, 734-760.
64. Heinsch, F.; Zhao, M., Running, S.; Kimball, J.; Nemani, R.; Davis, K.; Ricciuto, D.; Law, B.; Oechel, W.; Kwon, H.; Munger, J.; Baldocchi, D.; Xu, L.; Hollinger, D.; Richardson, A.; Stoy, P.; Siquerira, M.; Monson, R.; Burns, S.; Flanagan, L. Evaluation of remote sensing based terrestrial productivity from MODIS using regional tower eddy flux network observations. *IEEE Transactions on Geoscience and Remote Sensing* **2006**, *44*, 1908-1925.
65. Wylie, B.; Johnson, D.; Laca, E.; Saliendra, N.; Gilmanov, T.; Reed, B.; Tieszen, L.; Worstell, B. Calibration of remotely sensed, coarse resolution NDVI to CO_2 fluxes in a sagebrush-steppe ecosystem. *Remote Sensing of Environment* **2003**, *85*, 243-255.
66. Huete, A.; Didan, K.; Shimabakuro,Y.; Ratana, P.; Saleska, S.; Hutyra, L.; Yang, W.; Nemani, R.; Myneni, R. Amazon rainforest green-up with sunlight in dry season. *Geophysical Research Letters* **2006**, *33*, L06405.
67. Saleska, S.; Didan, K.; Huete, A.; da Rocha, R. Amazon forests green-up during 2005 drought. *Science* **2007**, *318*, 612.
68. Huete, A.; Restrepo-Coupe, N.; Ratana, P.; Didan, K.; Saleska, S.; Ichii, K.; Panuthai, S.; Gamo, M. Multiple site tower flux and remote sensing comparisons of tropical forest dynamics in monsoon Asia. *Agricultural and Forest Meteorology* **2008** (in press).
69. Sims, D.; Rahman, A.; Cordova, V.; El-Masria, B.; Baldocchi, D.; Flanagan, L.; Goldstein, A.; Hollinger, D.; Misson, L.; Schmid, H.; Wofsy, S.; Xu, L. On the use of MODIS EVI to assess

gross primary productivity of North American ecosystems. *Journal of Geophysical Research – Biogeosciences* **2006**, *111*, Art. No. G04015.

70. Rahman, A.; Sims, D.; Cordova, V.; El-Masri, B. Potential of MODIS EVI and surface temperature for directly estimating per-pixel ecosystem C fluxes. *Geophysical Research Letters* **2005**, *32*, 10.1029/2005GL024127.
71. Yuan, W.; Liu, S.; Zhou, G.; Zhou, G.Y.; Tieszen, L.; Baldochhi, D., Bernhofer, C.; Cholz, H., Godstein, A.; Goulden, M.; Hollinger, D.; Hu, Y.; Law, B.; Stoy, P.; Vesala, T.; Wofsy, S. Deriving a light use efficiency model from eddy covariance flux data for predicting daily gross primary production across biomes. *Agricultural and Forest Metoerology* **2007**, *143*, 189-207.
72. Xiao, X.; Zhang, Q.; Braswell, B.; Urbanski, S.; Boles, I.; Wofsy, S.; Moore, B.; Ojima, D. Modeling gross primary production of temperate deciduous broadleaf forest using satellite images and climate data. *Remote Sensing of Environment* **2004**, *91*, 256-270.
73. Jenkins, J.; Richardson, A.; Braswell, B.; Ollinger, S.; Hollinger, D.; Smith, M. Refining light-use efficiency calculations for a deciduous forest canopy using simultaneous tower-based carbon flux and radiometric measurements. *Agricultural and Forest Meteorology* **2007**, *143*, 64-79.
74. Grace, J.; Nichol, C.; Disney, M.; Lewis, P.; Quaife, T.; Bowyer, P. Can we measure terrestrial photosynthesis from space directly, using spectral reflectance and flourescence? *Global Change Biology* **2007**, *13*, 1484-1497.
75. Carlson, T. An overview of the "triangle method" for estimating surface evapotranspiration and soil moisture from satellite imagery. *Sensors* **2007**, *7*, 1612-1629.
76. Nagler, P.; Glenn, E.; Kim, H.; Emmerich, W.; Scott, R.; Huxman, T.; Huete, A. Relationship between evapotranspiration and precipitation pulses in a semiarid rangeland estimated by moisture flux towers and MODIS vegetation indices. *Journal of Arid Environments* **2007**, *70*, 443-462.
77. Cleugh, H.; Leuning, R.; Mu, Q.; Running, S. Regional evaporation estimates from flux tower and MODIS satellite data. *Remote Sensing of Environment* **2007**, *106*, 285-304.
78. Mu, Q.; Heinsch, F.; Zhao, M.; Running, S. Development of a global evapotranspiration algorithm based on MODIS and global meteorology data. *Remote Sensing of Environment* **2007**, *111*, 519-536.
79. Yang, F.; White, M.; Michaelis, A.; Ichii, K.; Hashimoto, H.; Votava, P.; Zhu, H.; and Nemani, R. Prediction of continental-scale evapotranspiration by combining MODIS and Ameriflux data through support vector machine. *IEEE Transactions on Geoscience and Remote Sensing* **2006**, *44*, 3452-3461.
80. Wang, K.; Wang, P.; Li, Z.; Cribb, M.; Sparrow, M. A simple method to estimate actual evapotranspiration from a combination of net radiation, vegetation index, and temperature. *Journal of Geophysical Research – Atmospheres* **2007**, ***12***, Art. No. D15107.
81. Groeneveld, D.; Baugh, W.; Sanderson, J.; Cooper, D. Annual groundwater evapotranspiration mapped from single satellite scenes. *Journal of Hydrology* **2007**, *344*, 146-156.
82. Beven, K. A manifesto for the equifinality thesis. *Journal of Hydrology* **2006**, *320*, 18-36.
83. Swinburne, R. *Simplicity as Evidence for Truth*; Marquette University Press: Marquette, MI. **1997**.

84. Falge, E.; Reth, S.; Bruggemann, N.; Butterbach-Bahl, K.; Goldberg, V.; Oltchev, A.; Schaaf, S.; Spindler, G.; Spiller, B.; Queck, R.; Kostner, B.; Bernhofer, C. Comparison of surface energy exchange models with eddy flux data in forest and grassland ecosystems of Germany. *Ecological Modeling* **2005**, *188*, 174-216.

© 2008 by MDPI (http://www.mdpi.org). Reproduction is permitted for noncommercial purposes.